去泛素化酶USP30通过调控MFN2泛素化减轻脑出血所致脑损伤

赵静，蒋正，陈春丽

(中南大学湘雅二医院神经内科，长沙 410011)

[摘 要] 目的：脑出血是一种致残率和病死率均较高的脑卒中类型。线粒体功能障碍在脑出血后继发性脑损伤中发挥重要作用，保护线粒体功能被认为是一种潜在的治疗策略。泛素特异性蛋白酶30(ubiquitin-specific protease 30，USP30)是一种定位于线粒体外膜的去泛素化酶，在调控线粒体稳态中具有重要作用。本研究旨在探讨USP30在脑出血后的作用及其潜在分子机制。**方法：**采用血红素诱导的SH-SY5Y细胞模型和IV型胶原酶诱导的大鼠脑出血模型开展体内外实验。体外实验：将SH-SY5Y细胞分为对照组、血红素处理24 h组和血红素处理48 h组，采用蛋白质印迹法和免疫共沉淀(co-immunoprecipitation，Co-IP)检测线粒体融合蛋白质2(mitofusin 2，MFN2)表达及其泛素化水平。为验证USP30过表达效率，将未接受血红素处理的SH-SY5Y细胞分别转染空载体或USP30-Flag质粒48 h，分为control+vector组和control+USP30组，采用蛋白质印迹法检测USP30蛋白表达。随后将细胞分为对照组、血红素组、血红素+空载体组和血红素+USP30过表达组，后2组均在USP30-Flag质粒或空载体转染48 h后给予血红素处理。采用细胞计数试剂盒8法检测细胞活力，采用三磷酸腺苷(adenosine triphosphate，ATP)、活性氧(reactive oxygen species，ROS)及MitoSOX试剂盒评估线粒体功能，采用Mito-Tracker染色和透射电子显微镜观察线粒体形态，并采用蛋白质印迹法和Co-IP检测相关蛋白质表达及MFN2泛素化水平。体内实验：将大鼠分为假手术组和脑出血3 d组，采用蛋白质印迹法和Co-IP检测血肿周围组织中MFN2表达及其泛素化水平。随后将大鼠分为假手术组、脑出血组、脑出血+腺相关病毒(adeno-associated virus，AAV)-NC组和脑出血+AAV-USP30组，后2组均于脑出血建模前20 d经侧脑室注射AAV-USP30或AAV-NC。于脑出血后第3天采用改良Garcia评分评估神经功能，采用苏木精-伊红(hematoxylin and eosin，HE)和末端脱氧核苷酸转移酶dUTP缺口末端标记法(terminal deoxynucleotidyl transferase dUTP nick end labeling，TUNEL)染色评估组织学损伤及细胞凋亡，采用ATP和ROS水平检测、ATP5H免疫荧光和透射电子显微镜分别评估线粒体功能和超微结构，并采用蛋白质印迹法和Co-IP检测相关蛋白质表达及线粒体MFN2泛素化水平。**结果：**体外实验中，与对照组相比，血红素处理24和48 h后，SH-SY5Y细胞中MFN2泛素化水平显著升高，而MFN2蛋白表达显著降低(均P<0.01)。与血红素+空载体组相比，USP30过表达显著提高SH-SY5Y细胞活力，降低细胞内ROS及线粒体ROS水平，增加ATP含量，并减轻线粒体碎片化及超微结构损伤(均P<0.05)。同时，USP30过表达降低MFN2泛素化水平、上调MFN2和B细胞淋巴瘤-2蛋白(B-cell lymphoma-2，Bcl-2)表达(均P<0.05)，下调Bcl-2相关X蛋白(Bcl-2-associated X protein，Bax)和cleaved caspase-3表达(均P<0.05)。体内实验中，与假手术组相比，脑出血后第3天大鼠血肿周围组织中MFN2泛素化水平显著升高，而MFN2蛋白表达显著降低(均P<0.01)。与脑出血+AAV-NC组相比，AAV-USP30显著改善神经功能缺损，减轻血肿周围组织学损伤，减少TUNEL阳性细胞(均P<0.05)；同时降低ROS水平，提高ATP含量和ATP5H表达水平，并改善线粒体肿胀、空泡化及嵴结构破坏。AAV-USP30还降低MFN2泛素化水平、上调MFN2和Bcl-2表达，并下调Bax及cleaved caspase-3表达(均P<0.05)。**结论：**脑出血急性期可伴随MFN2泛素化增强和蛋白质表达下降，可能参与线粒体结构和功能损伤。USP30通过抑制MFN2的泛素化及其降解，维持线粒体结构和功能完整性，从而减轻脑出血诱导的脑损伤。USP30可能是脑出血治疗的潜在分子靶点。

[关键词] 泛素特异性蛋白酶30；线粒体融合蛋白质2；脑出血；泛素化；线粒体功能；细胞凋亡

收稿日期(Date of reception)：2026-04-03

第一作者(First author)：赵静，Email: iamzhaojing@qq.com, ORCID: 0000-0002-5044-9354；蒋正，Email: zhengjiang187@csu.edu.cn, ORCID: 0000-0002-1345-9553

通信作者(Corresponding author)：陈春丽，副研究员，Email: 168202083@csu.edu.cn, ORCID: 0000-0002-7391-8774

基金项目(Foundation item)：国家自然科学基金(82101542)；湖南省自然科学基金(2024JJ9106)。This work was supported by the National Natural Science Foundation (82101542) and the Natural Science Foundation of Hunan Province (2024JJ9106), China.

开放获取(Open access)：本文遵循知识共享许可协议，允许第三方用户按照署名-非商业性使用-禁止演绎4.0(CC BY-NC-ND 4.0)的方式，在任何媒介以任何形式复制、传播本作品(https://creativecommons.org/licenses/by-nc-nd/4.0/)。

©Journal of Central South University (Medical Science). All rights reserved.

Deubiquitinase USP30 alleviates brain injury after intracerebral hemorrhage by regulating MFN2 ubiquitination

ZHAO Jing, JIANG Zheng, CHEN Chunli

(Department of Neurology, Second Xiangya Hospital, Central South University, Changsha 410011, China)

ABSTRACT

Objective: Intracerebral hemorrhage (ICH) is a type of stroke associated with high rates of disability and mortality. Mitochondrial dysfunction plays an important role in secondary brain injury following ICH, and preservation of mitochondrial function is considered a potential therapeutic strategy. Ubiquitin-specific protease 30 (USP30) is a deubiquitinase located on the outer mitochondrial membrane and plays an important role in regulating mitochondrial homeostasis. This study aims to investigate the role of USP30 after ICH and its potential molecular mechanisms.

Methods: In vitro and in vivo experiments were conducted using a hemin-induced SH-SY5Y cell model and a type IV collagenase-induced rat model of ICH. For the in vitro experiments, SH-SY5Y cells were divided into a control group, a 24-h hemin treatment group, and a 48-h hemin treatment group. Western blotting and co-immunoprecipitation (Co-IP) were performed to determine the expression and ubiquitination levels of mitofusin 2 (MFN2). To verify USP30 overexpression efficiency, SH-SY5Y cells not exposed to hemin were transfected with either an empty vector or a USP30-Flag plasmid for 48 h, designated as the control+vector and control+USP30 groups, respectively, and USP30 protein expression was examined by Western blotting. Subsequently, cells were divided into a control group, a hemin group, a hemin+vector group, and a hemin+USP30-overexpression group. In the latter 2 groups, cells were treated with hemin 48 hours after transfection with USP30-Flag plasmid or empty vector, respectively. Cell viability was assessed using the cell counting kit-8 (CCK-8) assay. Mitochondrial function was evaluated using adenosine triphosphate (ATP), reactive oxygen species (ROS), and MitoSOX assay kits. Mitochondrial morphology was examined using Mito-Tracker staining and transmission electron microscopy. Western blotting and Co-IP were used to detect the expression of related proteins and the ubiquitination level of MFN2. For the in vivo experiments, rats were divided into a sham-operated group and a 3-day ICH group. Western blotting and Co-IP were performed to determine MFN2 expression and ubiquitination in perihematomal tissues. Subsequently, the rats were divided into a sham-operated group, an ICH group, an ICH plus negative-control AAV (AAV-NC) group, and an ICH plus adeno-associated virus expressing USP30 (AAV-USP30) group. In the latter 2 groups, adeno-associated virus (AAV)-USP30 or AAV-NC was injected into the lateral ventricle 20 days before ICH induction. On day 3 after ICH, neurological function was assessed using the modified Garcia score. Histological injury and apoptosis were evaluated using hematoxylin

©Journal of Central South University (Medical Science). All rights reserved.

and eosin (HE) and terminal deoxynucleotidyl transferase dUTP nick end labeling (TUNEL) staining. Mitochondrial function and ultrastructure were assessed by measuring ATP and ROS levels, ATP5H immunofluorescence, and transmission electron microscopy. Western blotting and Co-IP were used to determine the expression of related proteins and the ubiquitination level of mitochondrial MFN2.

Results: In the in vitro experiments, compared with the control group, SH-SY5Y cells treated with hemin for 24 or 48 h exhibited significantly increased MFN2 ubiquitination and significantly decreased MFN2 protein expression (all $P<0.01$). Compared with the hemin plus empty-vector group, USP30 overexpression significantly increased SH-SY5Y cell viability, reduced intracellular and mitochondrial ROS levels, increased ATP content, and alleviated mitochondrial fragmentation and ultrastructural damage (all $P<0.05$). Moreover, USP30 overexpression reduced MFN2 ubiquitination, upregulated the expression of MFN2 and B-cell lymphoma 2 (Bcl-2) (all $P<0.05$), and downregulated the expression of Bcl-2-associated X protein (Bax) and cleaved caspase-3 (all $P<0.05$). In the in vivo experiments, compared with the sham-operated group, rats exhibited significantly increased MFN2 ubiquitination and significantly decreased MFN2 protein expression in perihematomal tissues on day 3 after ICH (all $P<0.01$). Compared with the ICH plus AAV-NC group, AAV-USP30 significantly ameliorated neurological deficits, attenuated histological injury in perihematomal tissues, and reduced the number of TUNEL-positive cells (all $P<0.05$). AAV-USP30 also reduced ROS levels, increased ATP content and ATP5H expression, and ameliorated mitochondrial swelling, vacuolization, and cristae disruption. Furthermore, AAV-USP30 reduced MFN2 ubiquitination, upregulated MFN2 and Bcl-2 expression, and downregulated Bax and cleaved caspase-3 expression (all $P<0.05$).

Conclusion: Acute ICH is accompanied by increased MFN2 ubiquitination and decreased MFN2 protein expression, which may contribute to mitochondrial structural and functional impairment. USP30 preserves mitochondrial structural and functional integrity by suppressing MFN2 ubiquitination and degradation, thereby alleviating ICH-induced brain injury. USP30 may therefore represent a potential molecular target for the treatment of ICH.

KEY WORDS ubiquitin-specific protease 30; mitofusin 2; intracerebral hemorrhage; ubiquitination; mitochondrial function; apoptosis

脑出血是一种起病急骤、病死率和致残率均较高的严重脑卒中类型，给患者和社会带来沉重负担。尽管脑出血仅占全球所有脑卒中的10%~15%，但其导致的脑卒中相关残疾负担却超过50%[1]。脑出血可导致2种类型的脑损伤：由血肿形成或扩大引起的原发性损伤，以及在此基础上发生的继发性损伤[2]。初始血肿大小及其进展是影响脑出血后原发性脑损伤的关键因素[3]。继发性脑损伤则由原发性损伤触发的一系列病理生理过程所致，是病情恶化的主要原因。研究[4-5]表明，脑出血后的继发性脑损伤受到神经炎症、氧化应激及细胞凋亡等因素的共同驱动，这些因素均显著影响患者的预后。因此，减轻继发性脑损伤对改善脑出血患者的预后和生活质量至关重要。近年来，大量研究[6-7]强调，血肿周围区域的能量代谢紊乱是脑出血后损伤级联反应的主要驱动因素，最终可导致神经元凋亡。因此，针对脑出血后神经

©Journal of Central South University (Medical Science). All rights reserved.

元细胞的能量代谢功能障碍进行干预已成为减轻继发性脑损伤、改善患者预后的关键策略。

线粒体是关键的细胞器，能响应多种信号合成三磷酸腺苷(adenosine triphosphate，ATP)并维持能量稳态，以适应细胞环境和生理状态的变化[8]。作为有氧呼吸和能量产生的主要场所，线粒体在细胞代谢中发挥核心作用，其结构和功能受损与代谢紊乱直接相关。线粒体功能障碍是脑出血后继发性脑损伤发生的重要因素[9]，维持线粒体稳态对减轻脑出血后的继发性脑损伤至关重要[10-11]。近年来，线粒体动力学在调控线粒体结构与功能方面的作用日益受到关注[12]。线粒体分裂与融合是线粒体动力学调控的核心过程，其中多种鸟苷三磷酸(guanosine triphosphate，GTP)酶[如动力相关蛋白质1(dynamin-related protein 1，DRP1)、线粒体融合蛋白质1(mitofusin 1，MFN1)、线粒体融合蛋白质2(mitofusin 2，MFN2)和视神经萎缩蛋白质1(optic atrophy 1，OPA1)]发挥关键作用[13]。DRP1是调控线粒体裂变的关键因子，而MFN1、MFN2及OPA1则在维持线粒体融合过程中发挥重要作用[14]。在众多相关蛋白质中，MFN2是一种定位于线粒体外膜的动力蛋白质样GTP酶，其功能在中枢神经系统中备受关注。研究[15]发现，MFN2缺失可导致神经元线粒体碎片化，损害线粒体氧化呼吸链功能并破坏能量生成。此外，在皮层和海马中敲除MFN2会导致过度氧化应激和神经元细胞死亡[16]。相反，MFN2过表达在缺血再灌注损伤模型中表现出明显的神经保护作用，可减少缺血或缺氧诱导的神经元凋亡[17-18]。然而，MFN2是否能够作为减轻脑出血后神经元损伤的潜在治疗靶点，仍有待进一步阐明。

泛素特异性蛋白酶30(ubiquitin-specific protease 30，USP30)是一种定位于线粒体外膜的去泛素化酶[19]，可在一定程度上保护线粒体和过氧化物酶体免受损伤[20]。在氧糖剥夺/复氧(oxygen-glucose deprivation/reoxygenation，OGD/R)条件下，USP30能够抑制线粒体裂解，并阻止MFN2的泛素化及其降解[21]。然而，USP30在脑出血中的具体作用及其对脑出血后线粒体功能障碍的影响尚不明确。基于此，本研究拟探讨脑出血是否在体内和体外诱导MFN2的泛素化与降解，USP30过表达在脑出血体内外模型中是否能够减轻线粒体裂变，以及USP30是否通过调控MFN2的泛素化降解发挥神经保护作用。

1 材料与方法

1.1 伦理声明

本研究已获得中南大学动物护理与伦理审查委员会批准(审批号：2021117)。

1.2 实验动物

成年雄性SD大鼠(275~325 g)购自湖南斯莱克景达实验动物有限公司，饲养于湖南省人民医院中心实验室，环境条件受控(恒温25 ℃，相对湿度60%)。大鼠可自由获取食物和水，并维持12 h光照/12 h黑暗循环。实验过程中尽量减轻动物的痛苦。

1.3 体内脑出血模型的建立

参照文献[22]，采用注射IV型胶原酶的方法建立脑出血模型。简要步骤如下：大鼠经腹腔注射戊巴比妥钠(40 mg/kg)进行深度麻醉后，固定于立体定位仪上，经颅骨钻孔后将10 μL微量注射器插入右侧纹状体。随后，将溶解于2 μL 0.9%生理盐水中的IV型胶原酶0.2 U(货号C5138，美国Sigma公司)在10 min内缓慢注入。假手术组除以等体积生理盐水替代IV型胶原酶外，其余操作步骤相同。术后，将大鼠单笼饲养，让其自由摄食和饮水，注意保暖。

1.4 细胞培养与体外脑出血模型

SH-SY5Y细胞购于美国模式培养物集存库(American Type Culture Collection，ATCC)，培养于添加10%胎牛血清和1%青霉素-链霉素的杜氏改良Eagle培养基(Dulbecco's modified Eagle medium，DMEM)中，置于37 ℃、5% CO_2的湿润培养箱中。参照既往方案[23]，通过10 μmol/L血红素处理细胞24或48 h，建立体外脑出血模型。

1.5 实验分组

实验1：探讨脑出血对体内及体外MFN2及其泛素化水平的影响。将SH-SY5Y细胞分为对照组、血红素处理24 h组和血红素处理48 h组，分别检测细胞内MFN2及泛素化MFN2的蛋白表达水平。大鼠随机分为假手术组和脑出血3 d组。每组取同侧半球血肿周围组织，采用蛋白质印迹法和免疫共沉淀(co-immunoprecipitation，Co-IP)方法检测相关蛋白质表达(n=3)。

实验2：首先，为验证USP30质粒转染及过表达效率，SH-SY5Y细胞分别转染空载体质粒或USP30-Flag质粒48 h，即control+vector组和control+USP30组，采用蛋白质印迹法检测USP30蛋白表达(n=3)。

©Journal of Central South University (Medical Science). All rights reserved.

为进一步探讨USP30过表达是否能改善血红素诱导48 h后SH-SY5Y细胞的活力并减少线粒体损伤，将SH-SY5Y细胞分为4组：对照组、血红素组、血红素+空载体组、血红素+USP30过表达组。采用细胞计数试剂盒8(cell counting kit-8，CCK-8)法评估细胞活力。为确定过表达USP30能否减轻血红素诱导的线粒体损伤，采用Mito-Tracker染色和透射电子显微镜观察线粒体形态变化。进一步采用ATP检测试剂盒和ROS检测试剂盒评估线粒体功能。

实验3：探讨USP30过表达是否能改善脑出血动物模型的神经功能缺损、减轻组织学损伤、缓解线粒体功能障碍并减少血肿周围细胞凋亡。将大鼠随机分为4组：假手术组、脑出血组、脑出血+AAV-NC组、脑出血+AAV-USP30组。同时，在脑出血后第3天进行苏木精-伊红(hematoxylin and eosin，HE)和末端脱氧核苷酸转移酶dUTP缺口末端标记法(terminal deoxynucleotidyl transferase dUTP nick end labeling，TUNEL)染色，以评估细胞凋亡及组织学损伤(n=3)。此外，通过检测ROS水平、ATP含量及ATP合酶亚基ATP5H表达来评估线粒体功能。进一步采用透射电子显微镜观察线粒体超微结构变化，以评价USP30过表达对脑出血后线粒体形态的影响。

实验4：探讨USP30过表达在脑出血后发挥神经保护作用的潜在分子机制。将SH-SY5Y细胞分为4组：对照组、血红素组、血红素+空载体组、血红素+USP30过表达组。大鼠随机分为4组：假手术组、脑出血组、脑出血+AAV-NC组、脑出血+AAV-USP30组。通过蛋白质印迹法检测凋亡相关蛋白质的表达(n=3)。通过Co-IP分析评估每组中MFN2和泛素化MFN2的表达(n=3)。

1.6 体外USP30质粒转染

USP30-Flag质粒及空载体质粒购自中国长沙HonorGene公司(货号HG-HO032663)。按照Lipofectamine 3000转染试剂盒(货号L3000150，美国Invitrogen公司)说明书进行细胞转染。为验证转染效率，部分细胞在转染48 h后不进行血红素处理，直接收集用于USP30蛋白检测；其余细胞转染48 h后给予血红素处理，用于后续功能及机制实验。

1.7 腺相关病毒注射及行为学测试

在脑出血模型建立前20 d，将5 μL腺相关病毒(adeno-associated virus，AAV)-USP30或AAV-NC(购自中国上海GeneChem公司)缓慢注射至侧脑室。立体定位坐标以前囟为参考：后移1 mm，旁开中线1.5 mm，深度为硬膜下4.5 mm。采用微量注射泵以恒定速度进行注射，注射结束后将针头保留在原位10 min，以防止液体反流。假手术组在相同部位注射等体积无菌生理盐水。

于脑出血后第3天采用改良Garcia评分系统，包括自主活动、肢体对称性、前肢伸展、本体感觉、攀爬能力及触觉反应6项指标进行行为学评估，方法参照文献[24]。每项指标评分范围为0~3，总分为3~18，其中3分表示严重神经功能障碍，18分表示神经功能正常。所有行为学测试及评分均由2名独立研究人员在盲法条件下完成。

1.8 CCK-8测定

根据CCK-8(货号C0037，上海碧云天生物技术股份有限公司)说明书，按照1∶9的比例将CCK-8原液与基础培养基配制成CCK-8工作液，并将100 μL的CCK-8工作液分别加入每孔中，在37 ℃且避光条件下孵育1 h，使用多功能酶标仪在波长450 nm下检测各待测样品的吸光度值。细胞活力=(处理组吸光度值−空白孔吸光度值)/(对照组吸光度值−空白孔吸光度值)×100%。

1.9 蛋白质印迹法

采用含蛋白质酶和磷酸酶抑制剂混合物的放射免疫沉淀测定(radio-immunoprecipitation assay，RIPA)裂解液对SH-SY5Y细胞或血肿周围脑组织进行裂解并充分匀浆。匀浆后，样品经离心处理后，收集上清液。采用二喹啉甲酸(bicinchoninic acid，BCA)法测定蛋白质浓度，并将各组样品蛋白质浓度调整至一致。随后，将样品于95 ℃下加热10 min进行变性。蛋白质样品经十二烷基硫酸钠-聚丙烯酰胺凝胶电泳(sodium dodecyl sulfate-polyacrylamide gel electrophoresis，SDS-PAGE)分离后，转移至聚偏二氟乙烯(polyvinylidene fluoride，PVDF)膜上。采用5%脱脂奶粉室温封闭1 h后，将膜于4 ℃下分别与以下一抗孵育过夜：兔抗MFN2(1∶1 000，货号11925，美国Cell Signaling Technology公司)，小鼠抗ubiquitin(1∶1 000，货号3936，美国Cell Signaling Technology公司)，兔抗USP30(1∶1 000，货号15402-1-AP，武汉三鹰生物技术有限公司)，兔抗Bcl-2(1∶3 000，货号26593-1-AP，武汉三鹰生物技术有限公司)，兔抗Bax(1∶2 000，货号50599-2-Ig，武汉三鹰生物技术有限公司)，小鼠抗cleaved caspase-3(1∶1 000，货号66470-2-Ig，武汉三鹰生物技术有限公司)及小鼠抗β-actin(1∶5 000，货号66009-1-Ig，武汉三鹰生物技术有限公司)。一抗孵育结束后，加入相应的二抗，在室温下孵育90 min。最终采用ImageJ软件对蛋白

©Journal of Central South University (Medical Science). All rights reserved.

质条带进行定量分析。

1.10 Co-IP分析

将细胞或脑组织置于含蛋白质酶和磷酸酶抑制剂的RIPA裂解液中进行裂解，随后于4 ℃、20 000×*g*条件下离心30 min。收集上清液，加入蛋白质A/G于4 ℃下预清除4 h，以减少非特异性结合。随后，将样品分别与抗MFN2抗体或同种属IgG阴性对照在4 ℃下孵育过夜，以形成免疫复合物。孵育约12 h后，加入25 μL蛋白质A/G磁珠捕获免疫复合物，并于4 ℃下继续孵育4 h。孵育结束后，用免疫沉淀缓冲液洗涤磁珠5次。最后，加入1×SDS-PAGE上样缓冲液，在95 ℃下加热5 min以洗脱目标蛋白质，用于后续分析。

1.11 HE染色

大鼠用4%多聚甲醛灌注后，断头取脑。将大脑在4%多聚甲醛中固定24 h，石蜡包埋，切成4 μm厚的切片。切片用自来水冲洗，苏木精染色5 min，用0.1%盐酸乙醇溶液分化25 s，在磷酸盐缓冲液(phosphate-buffered saline，PBS)中返蓝45 min。然后用伊红复染5 min，95%乙醇脱水，中性树胶封片。根据是否存在完整或溶解的红细胞来识别血肿区域。

1.12 免疫荧光检测

脑切片与以下一抗孵育过夜：抗USP30(1∶200，货号15402-1-AP，武汉三鹰生物技术有限公司)和抗ATP5H(1∶200，货号PA5-92214，美国Invitrogen公司)。第2天，切片在避光条件下与相应的荧光染料偶联二抗孵育2 h，然后进行4',6-二脒基-2-苯基吲哚(4',6-diamidino-2-phenylindole，DAPI)染色。使用荧光显微镜观察染色情况。

1.13 Mito-Tracker染色

为观察线粒体形态，采用Mito-Tracker Green线粒体荧光探针(货号C1048，海门市碧云天生物技术研究所)进行染色。血红素处理后，将SH-SY5Y细胞与Mito-Tracker Green染料在37 ℃下孵育30 min，随后用PBS轻柔洗涤以去除未结合染料。最后，使用共聚焦激光扫描显微镜对细胞进行成像，并利用ImageJ软件对图像进行定量分析。对Mito-Tracker图像进行线粒体形态定量时，每组随机选取多个视野，统计具有连续管状线粒体和碎片化线粒体的细胞比例。线粒体呈短小点状或断裂分布者定义为碎片化线粒体，呈细长连续网络样分布者定义为相对正常线粒体。

1.14 TUNEL染色

将脑组织制备为厚10 μm的切片，采用TUNEL细胞凋亡检测试剂盒(货号C1086，中国上海翊圣生物科技有限公司)按照说明书进行染色。随后使用DAPI对细胞核进行复染。每张切片在荧光显微镜下随机选取4个视野进行观察。结果以400倍放大倍数下，每个视野中TUNEL阳性细胞占总细胞核数的百分比表示。

1.15 ATP水平检测

采用ATP检测试剂盒(货号A095-1-1，中国南京建成生物工程研究所)测定ATP水平。

1.16 细胞内ROS水平检测

使用半定量探针2',7'-二氯二氢荧光素二乙酸酯(2', 7'-dichlorodihydrofluorescein diacetate，DCFH-DA)按照说明书测量SH-SY5Y细胞和脑组织中的细胞内ROS水平。结果使用流式细胞仪记录。按ROS试剂盒(货号S0034，上海碧云天生物技术股份有限公司)说明书进行，以无血清DMEM培养基按1∶1 000的比例稀释DCFH-DA母液，配制成检测工作液。向样本中加入DCFH-DA工作液，在37 ℃培养箱中孵育20 min。随后使用无血清DMEM培养基洗涤细胞3次，以去除未进入细胞内的游离探针。最后采用流式细胞仪检测DCFH-DA荧光信号，并记录各组细胞平均荧光强度，以评价细胞内ROS水平。

1.17 SH-SY5Y细胞线粒体ROS检测

使用线粒体ROS荧光探针MitoSOX Green按照说明书检测SH-SY5Y细胞中的线粒体ROS水平。各组细胞经相应处理后，弃去培养液，使用胰酶消化并收集细胞，经PBS洗涤后加入终浓度为5 μmol/L的MitoSOX工作液重悬细胞，并置于37 ℃培养箱中避光孵育20 min。孵育结束后，使用预温无血清DMEM或PBS洗涤细胞3次，以去除游离探针。最后采用流式细胞仪检测MitoSOX荧光信号，并以平均荧光强度表示线粒体ROS水平。

1.18 透射电子显微镜观察线粒体超微结构

脑组织或SH-SY5Y细胞用2%戊二醛在磷酸钠缓冲液(0.1 mol/L，pH为7.4)中于4 ℃下预固定12 h。洗涤后，样品用1%锇酸固定2 h，然后用递增浓度的乙醇梯度脱水。将脱水后的样品转移至环氧丙烷中，包埋在Eponate 12树脂中，使用超薄切片机切成超薄切片(70 nm)。然后用醋酸铀染色切片，并使用透射电子显微镜拍摄显微照片。

©Journal of Central South University (Medical Science). All rights reserved.

1.19 统计学处理

采用GraphPad Prism 8.0软件进行统计学分析。符合正态分布的计量数据以均数±标准误表示，2组比较采用t检验，多组比较采用单因素方差分析和Tukey多重比较检验，P<0.05为差异有统计学意义。

2 结 果

2.1 脑出血诱导后MFN2表达及其泛素化水平的变化

血红素处理SH-SY5Y细胞24和48 h后，MFN2蛋白质表达均显著降低(P<0.01，图1A)，MFN2的泛素化水平显著升高(P<0.01，图1B)。与体外结果一致，脑出血诱导后第3天，大鼠脑组织中MFN2的表达明显下降(P<0.01，图1C)，而MFN2的泛素化水平则显著升高(P<0.01，图1D)。

2.2 过表达USP30减轻血红素诱导的细胞损伤及线粒体功能障碍

为验证USP30质粒转染及过表达效率，分别将空载体质粒或USP30-Flag质粒转染至未接受血红素处理的SH-SY5Y细胞。转染48 h后，结果(图2)显示，与control+vector组相比，control+USP30组细胞中USP30蛋白表达显著升高(P<0.05，图2A)。随后，进一步探讨过表达USP30对血红素诱导细胞损伤的保护作用。CCK-8结果显示，血红素处理显著降低了SH-SY5Y细胞活力(P<0.01，图2B)，而过表达USP30干预可明显提高细胞活力(P<0.05，图2B)。相反，血红素处理后细胞内ROS水平显著升高(P<0.01，图2F、2G)；而过表达USP30处理可显著降低ROS水平(P<0.01，图2F、2G)。同时，检测线粒体ROS和细胞内ATP含量评估线粒体功能。结果显示，血红素处理后线粒体ROS水平显著升高(P<0.01，图2D、2E)，ATP生成显著下降(P<0.01，图2C)；而过表达USP30处理可显著降低线粒体ROS水平(P<0.01，图2D、2E)，并提高ATP生成水平(P<0.05，图2C)。进一步通过Mito-Tracker Green染色观察线粒体形态变化。结果显示，血红素处理后SH-SY5Y细胞内大量线粒体发生明显碎片化(P<0.01，图2H、2I)；而USP30过表达后，具有正常细长管状线粒体的细胞比例显著增加(P<0.05，图2H、2I)。透射电子显微镜结果进一步证实，正常组细胞线粒体结构完整，嵴排列致密有序；而血红素组及血红素+空载体组线粒体明显肿胀、空泡化，嵴消失或断裂；相比之下，过表达USP30组线粒体仅表现为轻度肿胀和空泡化，部分嵴结构仍可见(图2J)。

2.3 过表达USP30改善脑出血诱导的神经功能损伤、细胞凋亡及线粒体损伤

通过脑室注射AAV-NC或AAV-USP30构建USP30过表达大鼠模型。免疫荧光结果显示，脑出血后第3天，AAV-USP30组血肿周围脑组织中USP30表达明显高于AAV-NC组(P<0.05，图3A、3B)，提示AAV转染成功。改良Garcia评分显示，脑出血大鼠于造模后第3天出现明显神经功能缺损(P<0.01，图3C)，而AAV-USP30处理可显著改善其神经功能(P<0.05，图3C)。HE染色显示，AAV-USP30处理可明显减轻血肿周围脑组织的组织学损伤(图3D)。另外，TUNEL染色结果表明，与脑出血+AAV-NC组相比，脑出血+AAV-USP30组TUNEL阳性细胞比例显著下降(P<0.01，图3E、3F)。

进一步检测了血肿周围组织ROS水平、ATP含量及ATP5H表达水平。结果显示，与假手术组相比，脑出血组和脑出血+AAV-NC组ROS水平显著升高(P<0.01，图4A、4B)，而AAV-USP30处理可显著降低脑出血后第3天的ROS水平(P<0.05，图4A、4B)。相反，脑出血组和脑出血+AAV-NC组ATP含量及ATP5H荧光强度均显著下降(均P<0.01，图4C、4D)，而AAV-USP30处理后ATP生成及ATP5H表达均显著升高(均P<0.05，图4C、4D)。透射电子显微镜结果进一步显示，假手术组线粒体呈规则椭圆形，嵴结构致密清晰，无明显空泡形成；而脑出血组及脑出血+AAV-NC组线粒体出现明显肿胀、空泡化及嵴断裂；AAV-USP30处理后上述线粒体超微结构损伤得到明显改善(图4F)。

2.4 过表达USP30通过抑制MFN2泛素化减少体内外MFN2降解

为进一步明确USP30是否参与调控MFN2泛素化，本研究检测了体内外模型中MFN2蛋白表达及其泛素化水平。体外实验显示，血红素处理后SH-SY5Y细胞中MFN2蛋白表达明显降低(P<0.01，图5A)，而MFN2泛素化水平升高(P<0.01，图5D)。USP30过表达后，MFN2蛋白表达显著恢复(P<0.01，图5A)，MFN2泛素化水平明显下降(P<0.05，图5D)。体内实验获得了相似结果：脑出血后第3天，血肿周围脑组织中MFN2表达下降、泛素化MFN2增加，而AAV-USP30处理可上调MFN2表达并降低其泛素化水平(图5B、5F)。

©Journal of Central South University (Medical Science). All rights reserved.

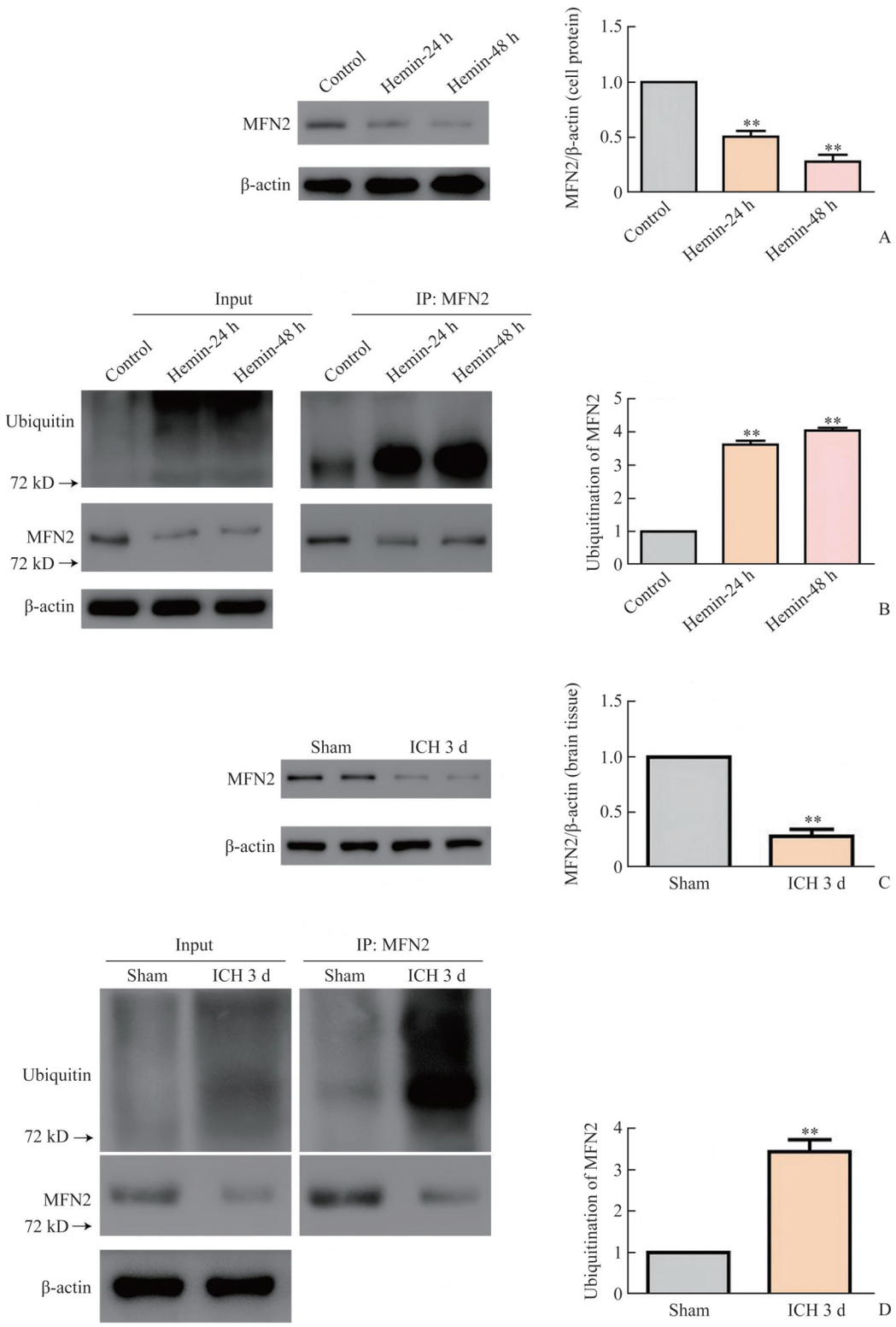


图1　MFN2及泛素化MFN2在脑出血大鼠和血红素诱导的SH-SY5Y细胞中的表达

Figure 1　Expression of MFN2 and ubiquitinated MFN2 in ICH rats and hemin-induced SH-SY5Y cells

A: Western blotting and quantification analysis of MFN2 in hemin-induced SH-SY5Y cells (n=3). B: Western blotting and quantification analysis of ubiquitinated MFN2 in hemin-induced SH-SY5Y cells (n=3). Values are indicated by mean±standard error, $^{**}P$<0.01 vs control. C: Western blotting and quantification analysis of MFN2 in an ICH animal model (n=3). D: Western blotting and quantification analysis of ubiquitinated MFN2 in ICH animal model (n=3). Values are indicated by mean±standard error. $^{**}P$<0.01 vs sham. MFN2: Mitofusin 2; ICH: Intracerebral hemorrhage.

©Journal of Central South University (Medical Science). All rights reserved.

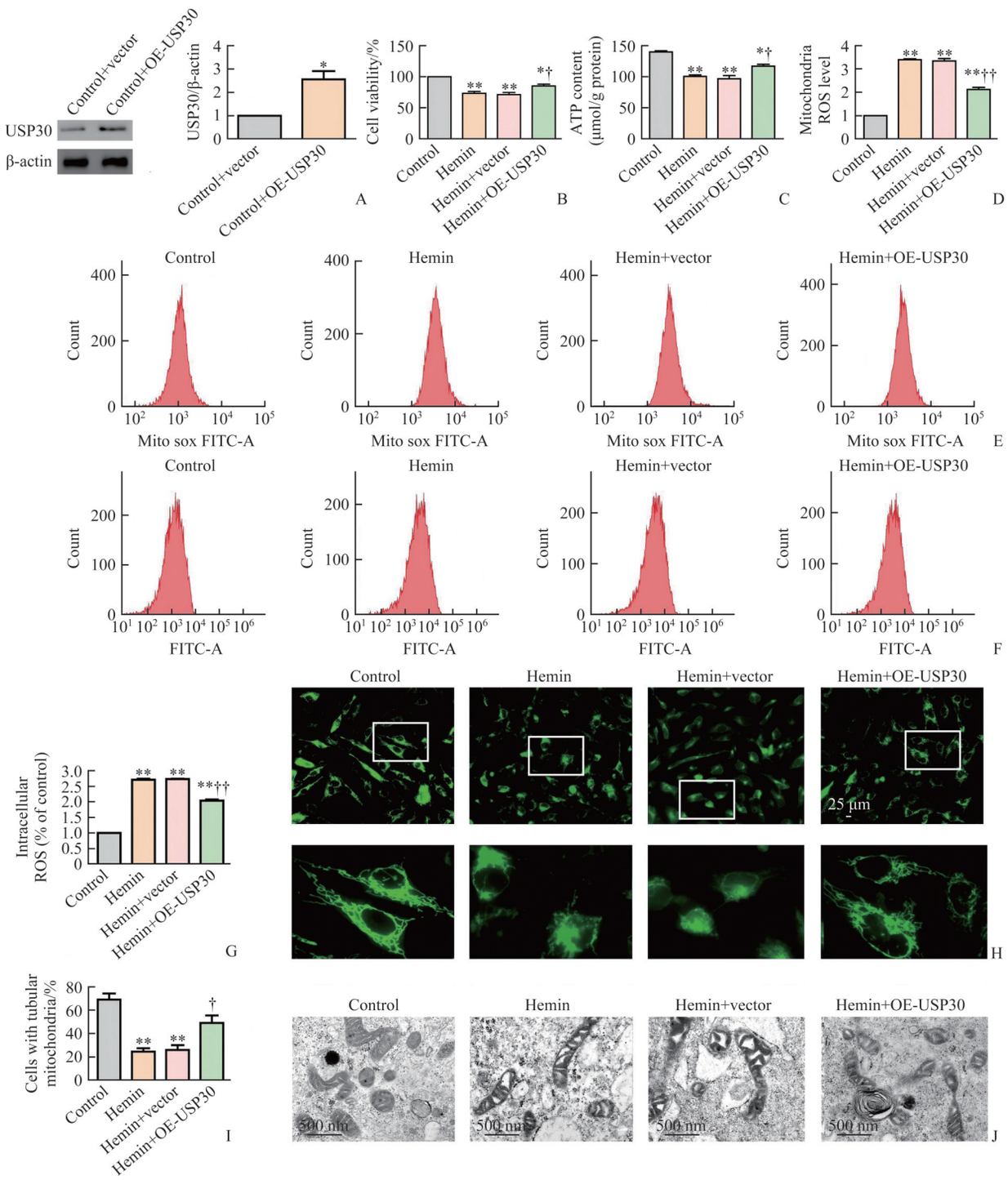


图2 过表达USP30改善血红素刺激引起的细胞死亡和线粒体损伤

Figure 2 Overexpression (OE)-USP30 ameliorates cell death and mitochondrial damage caused by hemin insult

A: Western blotting and quantitative analysis of USP30 expression in untreated SH-SY5Y cells transfected with empty vector or USP30-Flag plasmid for 48 h, corresponding to the control+vector and control+USP30 groups, respectively (n=3). B: Cellular viability assessed by the CCK8 assay in different experimental groups (n=3). C: ATP contents were assessed in various experimental groups using an ATP assay kit (n=3). D and E: Mitochondria ROS levels in various experimental groups were measured by MitoSOX staining (n=3). F and G: Intracellular ROS levels in various experimental groups were measured by staining with DCFH-DA staining (n=3); H and I: Variance of mitochondrial morphology was visualized with Mito-Tracker staining (n=3). J: Representative electron microscopic images of mitochondrial ultrastructure in SH-SY5Y cells. Values are indicated by mean± standard error. For A, *P<0.05, **P<0.01 vs control+vector; for B–J, *P<0.05, **P<0.01 vs control; †P<0.05, ††P<0.01 vs hemin+empty-vector. USP30: Ubiquitin-specific protease 30; ATP: Adenosine triphosphate; DCFH-DA: 2', 7'-Dichlorodihydrofluorescein diacetate; CCK8: Cell Counting Kit-8; ROS: Reactive oxygen species; FITC-A: FITC fluorescence intensity (area).

©Journal of Central South University (Medical Science). All rights reserved.

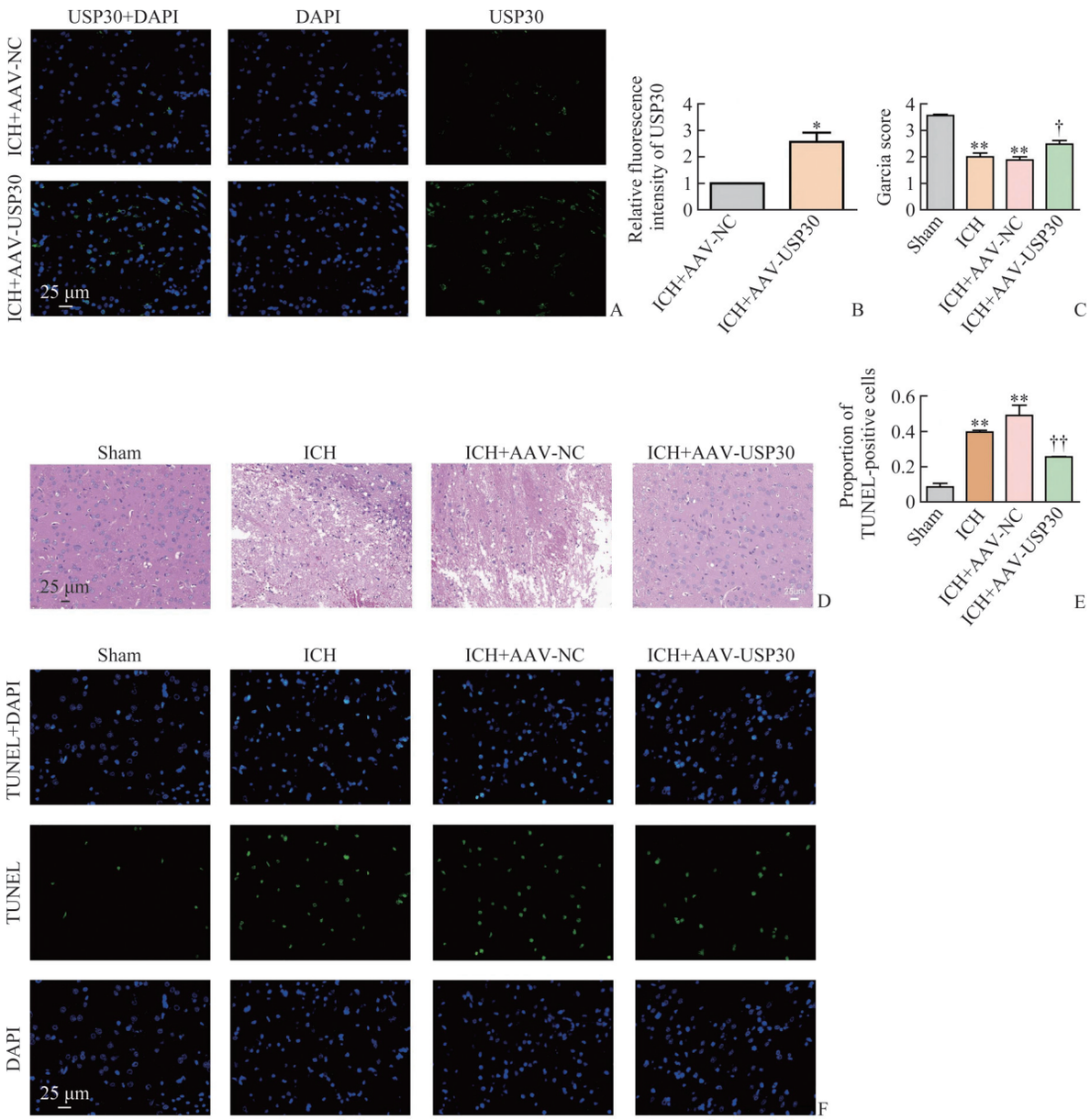


图3　过表达USP30改善脑出血诱导的病理损伤和细胞凋亡

Figure 3　OE-USP30 attenuates ICH-induced histopathological injury and apoptosis in rats

A and B: Representative immunofluorescence images (A) and quantitative analysis (B) of USP30 in rats (n=3). C: Neurological function assessed using the modified Garcia test (n=5). D: Representative images of histopathological changes evaluated by HE staining at 3 d after ICH (n=3). E and F: Quantitative analysis of the proportion of TUNEL-positive cells (E) and representative TUNEL staining images (F) in rats (n=3). Data are presented as mean±standard error. In B, *P<0.05 vs ICH+AAV-NC; in C and E, **P<0.01 vs sham, †P<0.05 and ††P<0.01 vs ICH+AAV-NC. DAPI: 4',6-diamidino-2-phenylindole; AAV: Adeno-associated virus; HE: Hematoxylin and eosin; TUNEL: Terminal deoxynucleotidyl transferase dUTP nick-end labeling.

2.5　过表达USP30下调Bax和cleaved caspase-3表达，同时上调Bcl-2表达

为明确过表达USP30的保护作用是否与抑制细胞凋亡有关，本研究采用蛋白质印迹法检测凋亡相关蛋白质Bcl-2、Bax及cleaved caspase-3的表达水平。体外实验结果显示，过表达USP30可显著降低血红素诱导的SH-SY5Y细胞中Bax和cleaved caspase-3的表达，同时显著上调Bcl-2蛋白质表达(均P<0.01，图6A~6D)。体内实验结果同样显示，与假手术组相比，脑出血组和脑出血+AAV-NC组中Bax和cleaved caspase-3表达均显著升高，而Bcl-2表达明显降低(均P<0.05)；相反，过表达USP30处理可显著下调Bax和cleaved caspase-3的表达，并上调Bcl-2的表达(均P<0.05，图6E~6H)。

©Journal of Central South University (Medical Science). All rights reserved.

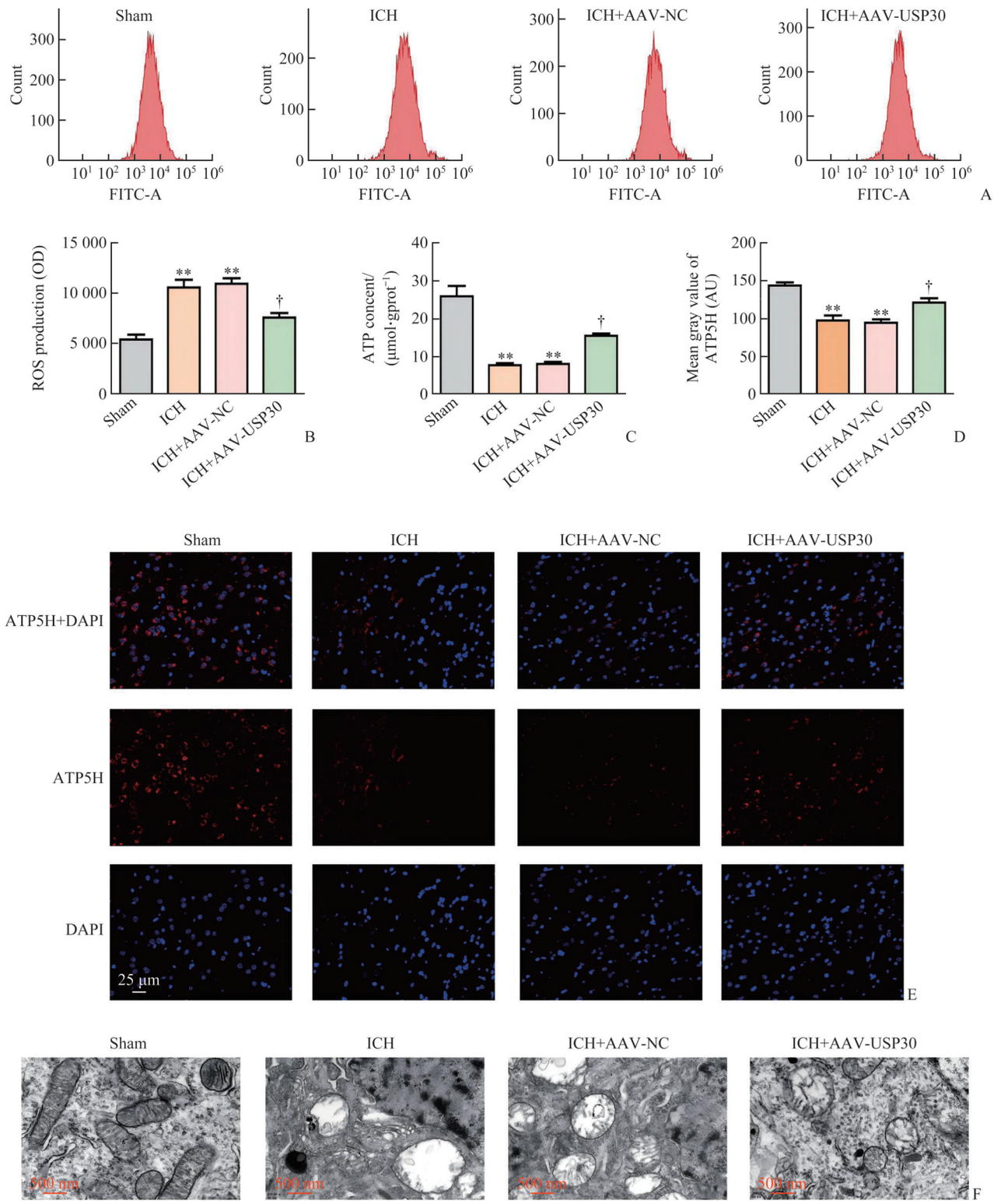


图4 过表达USP30改善脑出血诱导所致的线粒体功能与形态损伤

Figure 4 OE-USP30 improves mitochondrial function and ultrastructure in perihematomal tissue after ICH

A and B: Representative photographs and quantitative analysis of ROS levels in perihematomal tissue at 3 d after ICH (n=3). C: Quantitative analysis of ATP contents in perihematomal tissue at 3 d after ICH (n=3). D and E: Representative photographs and quantitative analysis of ATP5H expression in perihematomal tissue at 3 d after ICH (n=3). F: Representative electron microscopic images of mitochondrial ultrastructure in perihematomal tissue. Values are indicated by mean±standard error. **P<0.01 vs sham; †P<0.05 vs ICH+AAV-NC.

©Journal of Central South University (Medical Science). All rights reserved.

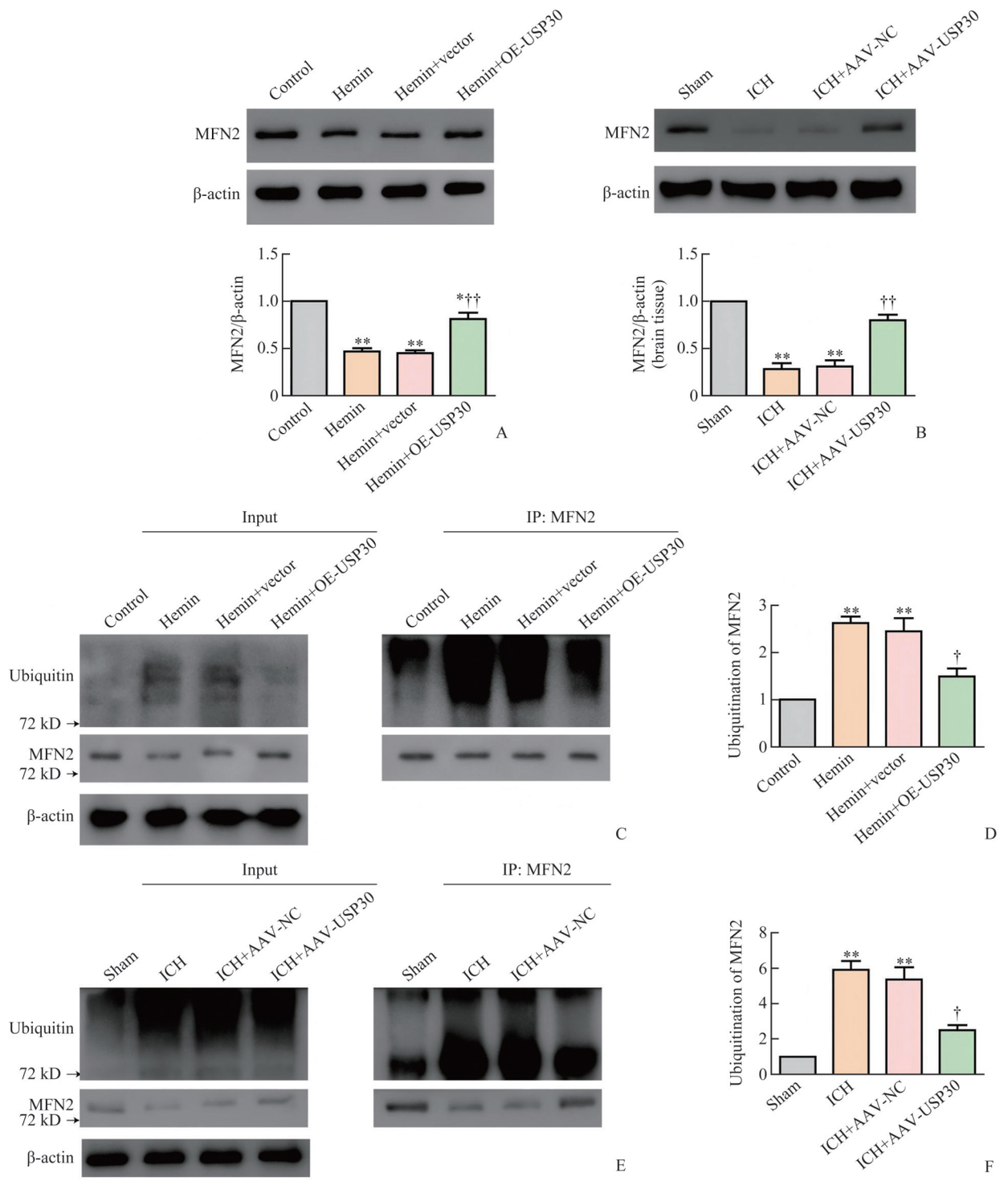


图5　过表达USP30对脑出血大鼠及血红素诱导的SH-SY5Y细胞中MFN2表达与MFN2泛素化水平的影响

Figure 5　Effects of OE-USP30 on MFN2 expression and MFN2 ubiquitination in ICH rats and hemin-induced SH-SY5Y cells

A: Western blotting and quantification analysis of MFN2 in in vitro groups (n=3). Values are indicated by mean±standard error. *P<0.05, **P<0.01 vs control; ††P<0.01 vs hemin+vector. B: Western blotting and quantification analysis of MFN2 in an animal model (n=3). Values are indicated by mean±standard error. **P<0.01 vs sham; ††P<0.01 vs ICH+AAV-NC. C and D: Western blotting and quantification analysis of ubiquitinated MFN2 in in vitro groups (n=3), **P<0.01 vs control; †P<0.05 vs hemin+vector. E and F: Western blotting (E) and quantification analysis (F) of ubiquitinated MFN2 in an ICH animal model (n=3). Values are indicated by mean±standard error. **P<0.01 vs sham; †P<0.05 vs ICH+AAV-NC.

©Journal of Central South University (Medical Science). All rights reserved.

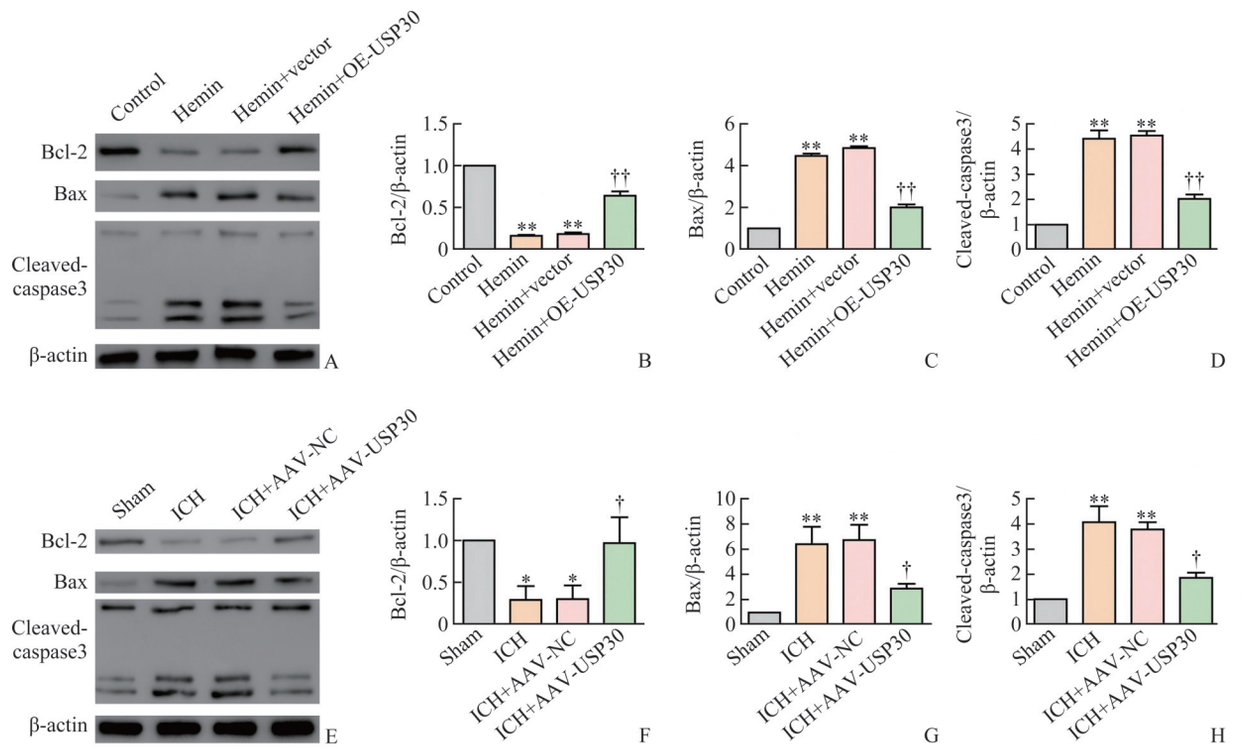


图6 过表达USP30下调Bax和cleaved-caspase-3表达并上调Bcl-2表达

Figure 6 OE-USP30 downregulates Bax and cleaved caspase-3 and upregulates Bcl-2 in vivo and in vitro

A－D: Western blotting and quantification analysis of Bax, cleaved-caspase3 and Bcl-2 in hemin-induced SH-SY5Y cells (n=3). Values are indicated by mean±standard error. **P<0.01 vs control; ††P<0.01 vs hemin+vector. E－H: Western blotting and quantification analysis of Bax, cleaved-caspase3 and Bcl-2 in ICH-induced rats (n=3). Values are indicated by mean±standard error. *P<0.05, **P<0.01 vs sham; †P<0.05 vs ICH+AAV-NC. Bax: Bcl-2-associated X protein; Bcl-2: B-cell lymphoma-2.

3 讨 论

本研究系统探讨了USP30在脑出血后早期脑损伤中的作用及其潜在分子机制。主要结果如下：1)胶原酶诱导的脑出血模型可明显增强MFN2的泛素化水平。在体外模型中，血红素处理24 h后，SH-SY5Y细胞中泛素化MFN2水平也明显升高；与此同时，在体内模型中，MFN2总蛋白质表达均明显下降，与其泛素化水平升高相对应。2)USP30过表达可改善脑出血大鼠的神经功能缺损，减轻组织学损伤，减少血肿周围细胞凋亡，并缓解线粒体功能障碍。3)USP30过表达可提高血红素处理48 h后SH-SY5Y细胞的活力，并减轻线粒体损伤。4)体内外实验均证实，USP30过表达通过抑制MFN2的泛素化从而稳定其蛋白质水平。5)USP30过表达在脑出血动物及细胞模型中可上调Bcl-2表达，同时下调Bax和cleaved caspase-3的表达。综上，USP30可能成为脑出血治疗的潜在干预靶点。

泛素-蛋白酶体系统(ubiquitin-proteasome system，UPS)是细胞内重要的蛋白质降解途径，负责调控细胞质、细胞核及跨膜蛋白质等多种蛋白质的降解过程，在神经系统发育及脑结构和功能维持中发挥关键作用[25-26]。此外，UPS也参与脑卒中后神经元损伤的发生、发展[27]。泛素化蛋白质的异常积聚是脑卒中的重要特征之一[28-29]。本研究首先分析了脑出血模型中线粒体外膜蛋白质MFN2的表达及其泛素化情况。结果显示，无论在体外血红素处理24 h，还是在体内脑出血建模后3 d，泛素化MFN2水平均显著升高，同时伴随MFN2总蛋白质表达水平下降。这提示，泛素化增强在脑出血后MFN2降解过程中发挥关键作用。MFN2的降解在其他神经系统疾病中也得到了广泛研究。例如，在蛛网膜下腔出血后24 h，同侧脑组织中MFN2表达显著降低[30]；Martorell-Riera等[15]发现N-甲基-D-天冬氨酸(N-methyl-D-aspartate，NMDA)处理后大鼠皮质神经元中MFN2水平下降；Klacanova等[31]报道脑缺血再灌注损伤后皮层中MFN2表达减少。上述研究提示，MFN2的降低可能参与多种脑损伤的病理过程。

靶向MFN2被视为在不同神经系统疾病治疗中靶向线粒体保护的一种有前景的策略。例如，MFN2激

©Journal of Central South University (Medical Science). All rights reserved.

动剂可逆转腓骨肌萎缩症2A型临床前模型中的线粒体缺陷[32]；大麻二酚通过抑制MFN2泛素化降解稳定其表达，从而减轻脑缺血再灌注损伤；人参皂苷化合物K通过抑制MFN2的泛素化降解，维持线粒体动力学和生物能量学稳定[33]；MFN2过表达还可缓解七氟烷诱导的认知功能障碍[34]。然而，MFN2在脑出血中的具体作用仍有待进一步阐明。

USP30作为USP家族成员，主要定位于线粒体外膜和过氧化物酶体[35]。USP30缺失可导致线粒体延长并呈网络状连接，而其过表达则可逆转该表型[36]。USP30能够去除线粒体上K6和K11连接的泛素链，并调节非典型泛素链[37]。研究[38]表明，USP30通过去泛素化MFN1和MFN2，抑制线粒体裂变。本研究进一步证实，过表达USP30可通过抑制MFN2的泛素化降解，减轻脑出血诱导的细胞凋亡。值得注意的是，USP30在不同神经系统疾病中的作用存在一定差异。例如，Bingol等[39]发现抑制USP30可通过增强parkin介导的线粒体自噬发挥神经保护作用；Liu等[40]报道USP30抑制剂在蛛网膜下腔出血中通过促进线粒体自噬发挥保护作用。相反，Imam Aliagan等[41]发现USP30过表达可减轻鱼藤酮诱导的多巴胺能神经元损伤。此外，USP30在OGD/R模型中亦表现出保护作用[21]。这些差异可能与实验模型、细胞类型及干预方式等因素有关。

线粒体是病理状态下ROS生成的主要来源，ROS积累是线粒体功能障碍的重要标志之一。ATP5H是线粒体内膜的重要组成部分，参与氧化磷酸化和ATP合成[42-43]。鉴于USP30通过调控MFN2泛素化在维持线粒体稳态中的重要作用[38]，本研究进一步分析了USP30对线粒体功能的影响。结果显示，过表达USP30可显著抑制MFN2泛素化并上调其表达，同时减轻ATP耗竭、减少ROS生成，并改善线粒体形态结构。体内实验亦得到一致结果，提示USP30可改善脑出血后线粒体生物能量代谢并维持其结构完整性。考虑到MFN2在调控线粒体融合及细胞器间通讯中的关键作用，推测其可能是USP30发挥保护作用的重要靶点。

细胞凋亡是脑出血后血肿周围组织早期损伤的重要机制。脑出血后，线粒体通透性转换孔开放导致细胞色素c释放，从而触发凋亡级联反应[44]。Bcl-2、Bax及cleaved caspase-3等蛋白质在该过程中发挥关键调控作用[45]。本研究发现，过表达USP30通过调节上述凋亡相关蛋白质的表达，显著减少细胞凋亡。结合其减少ROS及恢复ATP生成的作用，提示其抗凋亡效应可能与线粒体功能修复密切相关。

综上所述，本研究揭示了USP30可能通过抑制MFN2泛素化及其降解、改善线粒体稳态而发挥保护作用。然而，本研究仍存在一定局限性：1)主要关注脑出血后第3天急性期损伤，尚未评估USP30过表达对7、14或21 d长期神经功能恢复和组织修复的影响。因此，本研究结论主要适用于脑出血急性期线粒体损伤和细胞凋亡过程，USP30是否具有长期神经保护作用仍需进一步研究。2)采用USP30过表达策略验证其保护作用，但未进行USP30敲低或敲除实验，未来将进一步通过siRNA/shRNA、成簇规律间隔短回文重复序列/CRISPR相关蛋白9(clustered regularly interspaced short palindromic repeats/CRISPR-associated protein 9，CRISPR/Cas9)或条件性敲除动物验证USP30缺失是否加重MFN2降解和神经损伤。3)虽然USP30过表达可降低MFN2泛素化水平并上调MFN2表达，但尚未进行MFN2沉默及回复实验，因此不能证明MFN2是USP30发挥保护作用的唯一或必需中介。4)MFN2降解可能同时受到UPS和自噬-溶酶体系统调控。MFN2作为线粒体外膜蛋白质，其泛素化不仅可能导致蛋白酶体降解，也可能参与线粒体自噬相关的选择性清除。因此，本研究中观察到的MFN2泛素化升高和蛋白质下降并不能完全排除自噬-溶酶体途径参与的可能性。未来需结合蛋白酶体抑制剂、溶酶体抑制剂及线粒体自噬标志物进一步明确MFN2的降解机制[46-47]。5)部分分子生物学和组织学检测样本量相对有限，可能影响统计效能和结果稳定性。虽然各项指标在体内外实验中呈现一致趋势，但仍需在更大样本量及多时间点实验中进一步验证。此外，未来仍需采用谷胱甘肽-S-转移酶沉降实验、免疫荧光共定位等生物学方法进一步明确USP30是否直接结合MFN2及其作用位点。

作者贡献声明：赵静、蒋正　实验操作，数据分析，论文撰写；陈春丽　实验设计与指导，论文修改与审阅。所有作者阅读并同意最终的文本。

利益冲突声明：作者声称无任何利益冲突。

参考文献

[1] Zhao J, Chen C, Ge L, et al. TAK1 inhibition mitigates intracerebral hemorrhage-induced brain injury through reduction of oxidative stress and neuronal pyroptosis via the NRF2 signaling pathway[J]. Front Immunol, 2024, 15: 1386780. https://doi.org/10.3389/fimmu.2024.1386780.

[2] Liu Y, Qi L, Li Z, et al. Crosstalk between matrix metalloproteinases and their inducer EMMPRIN/CD147: a promising therapeutic target for intracerebral hemorrhage[J]. Transl Stroke Res, 2025, 16(2): 557-567. https://doi.org/10.

©Journal of Central South University (Medical Science). All rights reserved.

1007/s12975-023-01225-6.

[3] Deng X, Ren J, Chen K, et al. Mas receptor activation facilitates innate hematoma resolution and neurological recovery after hemorrhagic stroke in mice[J]. J Neuroinflammation, 2024, 21(1): 106. https://doi.org/10.1186/s12974-024-03105-8.

[4] Zille M, Farr TD, Keep RF, et al. Novel targets, treatments, and advanced models for intracerebral haemorrhage[J]. eBioMedicine, 2022, 76: 103880. https://doi.org/10.1016/j.ebiom.2022.103880.

[5] Xue M, Yong V. Neuroinflammation in intracerebral haemorrhage: immunotherapies with potential for translation [J]. Lancet Neurol, 2020, 19(12): 1023-1032. https://doi.org/10.1016/S1474-4422(20)30364-1.

[6] Chen W, Guo C, Feng H, et al. Mitochondria: novel mechanisms and therapeutic targets for secondary brain injury after intracerebral hemorrhage[J]. Front Aging Neurosci, 2021, 12: 615451. https://doi.org/10.3389/fnagi.2020.615451.

[7] He Q, Li Z, Li T, et al. Atp stimulation promotes functional recovery after intracerebral haemorrhage by increasing the mBDNF/proBDNF ratio[J]. Neuroscience, 2021, 459: 104-117. https://doi.org/10.1016/j.neuroscience.2020.12.034.

[8] Sreedhar A, Aguilera-Aguirre L, Singh KK. Mitochondria in skin health, aging, and disease[J]. Cell Death Dis, 2020, 11: 444. https://doi.org/10.1038/s41419-020-2649-z.

[9] Li X, Liu W, Jiang G, et al. Celastrol ameliorates neuronal mitochondrial dysfunction induced by intracerebral hemorrhage via targeting cAMP-activated exchange protein-1 [J]. Adv Sci, 2024, 11(19): 2307556. https://doi.org/10.1002/advs.202307556.

[10] Li Y, Liu H, Tian C, et al. Targeting the multifaceted roles of mitochondria in intracerebral hemorrhage and therapeutic prospects[J]. Biomed Pharmacother, 2022, 148: 112749. https://doi.org/10.1016/j.biopha.2022.112749.

[11] Gareev I, Beylerli O, Liang Y, et al. The role of mitochondria-targeting miRNAs in intracerebral hemorrhage[J]. Curr Neuropharmacol, 2023, 21(5): 1065-1080. https://doi.org/10.2174/1570159x20666220507021445.

[12] Wu Y, Hu Q, Wang X, et al. Pterostilbene attenuates microglial inflammation and brain injury after intracerebral hemorrhage in an OPA1-dependent manner[J]. Front Immunol, 2023, 14: 1172334. https://doi.org/10.3389/fimmu.2023.1172334.

[13] Ni HM, Williams JA, Ding WX. Mitochondrial dynamics and mitochondrial quality control[J]. Redox Biol, 2015, 4: 6-13. https://doi.org/10.1016/j.redox.2014.11.006.

[14] Chiurazzi M, Di Maro M, Cozzolino M, et al. Mitochondrial dynamics and microglia as new targets in metabolism regulation[J]. Int J Mol Sci, 2020, 21(10): 3450. https://doi.org/10.3390/ijms21103450.

[15] Martorell-Riera A, Segarra-Mondejar M, Muñoz JP, et al. Mfn2 downregulation in excitotoxicity causes mitochondrial dysfunction and delayed neuronal death[J]. EMBO J, 2014, 33 (20): 2388-2407. https://doi.org/10.15252/embj.201488327.

[16] Jiang S, Nandy P, Wang W, et al. Mfn2 ablation causes an oxidative stress response and eventual neuronal death in the hippocampus and cortex[J]. Mol Neurodegener, 2018, 13(1): 5. https://doi.org/10.1186/s13024-018-0238-8.

[17] Peng C, Rao W, Zhang L, et al. Mitofusin 2 ameliorates hypoxia-induced apoptosis via mitochondrial function and signaling pathways[J]. Int J Biochem Cell Biol, 2015, 69: 29-40. https://doi.org/10.1016/j.biocel.2015.09.011.

[18] Peng C, Rao W, Zhang L, et al. Mitofusin 2 exerts a protective role in ischemia reperfusion injury through increasing autophagy[J]. Cell Physiol Biochem, 2018, 46(6): 2311-2324. https://doi.org/10.1159/000489621.

[19] Wang Y, Serricchio M, Jauregui M, et al. Deubiquitinating enzymes regulate PARK2-mediated mitophagy[J]. Autophagy, 2015, 11(4): 595-606. https://doi.org/10.1080/15548627.2015.1034408.

[20] Riccio V, McQuibban GA, Kim PK. USP30: protector of peroxisomes and mitochondria[J]. Mol Cell Oncol, 2019, 6(3): 1600350. https://doi.org/10.1080/23723556.2019.1600350.

[21] Chen C, Qin H, Tang J, et al. USP30 protects against oxygen-glucose deprivation/reperfusion induced mitochondrial fragmentation and ubiquitination and degradation of MFN2[J]. Aging, 2021, 13(4): 6194-6204. https://doi.org/10.18632/aging.202629.

[22] Deng S, Hu Q, Chen X, et al. GM130 protects against blood-brain barrier disruption and brain injury after intracerebral hemorrhage by regulating autophagy formation[J]. Exp Gerontol, 2022, 163: 111772. https://doi.org/10.1016/j.exger.2022.111772.

[23] Peng C, Gong X, Hu Z, et al. Selective HDAC6 inhibitor *TubA* offers neuroprotection after intracerebral hemorrhage via inhibiting neuronal apoptosis[J/OL]. Peer J, 2023, 11: e15293 [2026-01-23]. https://doi.org/10.7717/peerj.15293.

[24] Garcia JH, Wagner S, Liu KF, et al. Neurological deficit and extent of neuronal necrosis attributable to middle cerebral artery occlusion in rats: statistical validation[J]. Stroke, 1995, 26(4): 627-635. https://doi.org/10.1161/01.str.26.4.627.

[25] Vriend J, Ghavami S, Marzban H. The role of the ubiquitin proteasome system in cerebellar development and medulloblastoma[J]. Mol Brain, 2015, 8(1): 64. https://doi.org/10.1186/s13041-015-0155-5.

[26] Jarome TJ, Helmstetter FJ. The ubiquitin-proteasome system as a critical regulator of synaptic plasticity and long-term memory formation[J]. Neurobiol Learn Mem, 2013, 105: 107-116. https://doi.org/10.1016/j.nlm.2013.03.009.

[27] Ge P, Luo Y, Liu CL, et al. Protein aggregation and proteasome dysfunction after brain ischemia[J]. Stroke, 2007, 38(12): 3230-3236. https://doi.org/10.1161/STROKEAHA.107.487108.

[28] Luo T, Park Y, Sun X, et al. Protein misfolding, aggregation, and autophagy after brain ischemia[J]. Transl Stroke Res, 2013, 4(6): 581-588. https://doi.org/10.1007/s12975-013-0299-5.

[29] Li Y, Wang Y, Zou W. Exploration on the mechanism of ubiquitin proteasome system in cerebral stroke[J]. Front Aging Neurosci, 2022, 14: 814463. https://doi.org/10.3389/fnagi.2022.

©Journal of Central South University (Medical Science). All rights reserved.

814463.

[30] Liu Y, Liu R, Huang L, et al. Inhibition of prostaglandin E2 receptor EP3 attenuates oxidative stress and neuronal apoptosis partially by modulating p38MAPK/FOXO3/Mul1/Mfn2 pathway after subarachnoid hemorrhage in rats[J]. Oxid Med Cell Longev, 2022, 2022: 7727616. https://doi.org/10.1155/2022/7727616.

[31] Klacanova K, Kovalska M, Chomova M, et al. Global brain ischemia in rats is associated with mitochondrial release and downregulation of Mfn2 in the cerebral cortex, but not the hippocampus[J]. Int J Mol Med, 2019, 43(6): 2420-2428. https://doi.org/10.3892/ijmm.2019.4168.

[32] Rocha AG, Franco A, Krezel AM, et al. MFN2 agonists reverse mitochondrial defects in preclinical models of Charcot-Marie-Tooth disease type 2A[J]. Science, 2018, 360(6386): 336-341. https://doi.org/10.1126/science.aao1785.

[33] Huang Q, Li J, Chen J, et al. Ginsenoside compound K protects against cerebral ischemia/reperfusion injury via Mul1/Mfn2-mediated mitochondrial dynamics and bioenergy[J]. J Ginseng Res, 2023, 47(3): 408-419. https://doi.org/10.1016/j.jgr.2022.10.004.

[34] Zhu R, Liu L, Mao T, et al. Mfn2 regulates mitochondria and mitochondria-associated endoplasmic reticulum membrane function in neurodegeneration induced by repeated sevoflurane exposure[J]. Exp Neurol, 2024, 377: 114807. https://doi.org/10.1016/j.expneurol.2024.114807.

[35] Wang F, Gao Y, Zhou L, et al. USP30: structure, emerging physiological role, and target inhibition[J]. Front Pharmacol, 2022, 13: 851654. https://doi.org/10.3389/fphar.2022.851654.

[36] Nakamura N, Hirose S. Regulation of mitochondrial morphology by USP30, a deubiquitinating enzyme present in the mitochondrial outer membrane[J]. MBoC, 2008, 19(5): 1903-1911. https://doi.org/10.1091/mbc.e07-11-1103.

[37] Cunningham CN, Baughman JM, Phu L, et al. USP30 and parkin homeostatically regulate atypical ubiquitin chains on mitochondria[J]. Nat Cell Biol, 2015, 17(2): 160-169. https://doi.org/10.1038/ncb3097.

[38] Hou J, Eldeeb M, Wang X. Beyond deubiquitylation: USP30-mediated regulation of mitochondrial homeostasis [M]//Mitochondrial DNA and Diseases. Singapore: Springer Singapore, 2017: 133-148. https://doi.org/10.1007/978-981-10-6674-0_10.

[39] Bingol B, Tea JS, Phu L, et al. The mitochondrial deubiquitinase USP30 opposes parkin-mediated mitophagy[J]. Nature, 2014, 510(7505): 370-375. https://doi.org/10.1038/nature13418.

[40] Liu Y, Yao C, Sheng B, et al. Inhibition of USP30 promotes mitophagy by regulating ubiquitination of MFN2 by parkin to attenuate early brain injury after SAH[J]. Transl Stroke Res, 2025, 16(2): 448-466. https://doi.org/10.1007/s12975-023-01228-3.

[41] Imam Aliagan AD, Ahwazi MD, Tombo N, et al. Parkin interacts with Mitofilin to increase dopaminergic neuron death in response to Parkinson's disease-related stressors[J]. Am J Transl Res, 2020, 12(11): 7542-7564.

[42] Bernardi P, Di Lisa F, Fogolari F, et al. From ATP to PTP and back: a dual function for the mitochondrial ATP synthase[J]. Circ Res, 2015, 116(11): 1850-1862. https://doi.org/10.1161/circresaha.115.306557.

[43] Zhao W, Wang H, Liu J, et al. Mitochondrial respiratory chain complex abnormal expressions and fusion disorder are involved in fluoride-induced mitochondrial dysfunction in ovarian granulosa cells[J]. Chemosphere, 2019, 215: 619-625. https://doi.org/10.1016/j.chemosphere.2018.10.043.

[44] Wang Z, Zhou F, Dou Y, et al. Melatonin alleviates intracerebral hemorrhage-induced secondary brain injury in rats via suppressing apoptosis, inflammation, oxidative stress, DNA damage, and mitochondria injury[J]. Transl Stroke Res, 2018, 9(1): 74-91. https://doi.org/10.1007/s12975-017-0559-x.

[45] Lončarević-Vasiljković N, Milanović D, Pešić V, et al. Dietary restriction suppresses apoptotic cell death, promotes Bcl-2 and Bcl-xl mRNA expression and increases the Bcl-2/Bax protein ratio in the rat cortex after cortical injury[J]. Neurochem Int, 2016, 96: 69-76. https://doi.org/10.1016/j.neuint.2016.02.017.

[46] Sun-Wang JL, Ivanova S, Zorzano A. The dialogue between the ubiquitin-proteasome system and autophagy: Implications in ageing[J]. Ageing Res Rev, 2020, 64: 101203. https://doi.org/10.1016/j.arr.2020.101203.

[47] Wu M, Lu G, Lao YZ, et al. Garciesculenxanthone B induces PINK1-Parkin-mediated mitophagy and prevents ischemia-reperfusion brain injury in mice[J]. Acta Pharmacol Sin, 2021, 42(2): 199-208. https://doi.org/10.1038/s41401-020-0480-9.

（责任编辑　彭敏宁）

©Journal of Central South University (Medical Science). All rights reserved.